Revista Brasileira de Recursos Hídricos
Brazilian Journal of Water Resources
Versão On-line ISSN 2318-0331
RBRH, Porto Alegre, v. 22, e23, 2017
Scientific/Technical Article

http://dx.doi.org/10.1590/2318-0331.011716058

Principle of maximum entropy in the estimation of suspended sediment concentration

Princípio da entropia máxima na estimativa da concentração de sedimentos em suspensão

Patrícia Diniz Martins[1] and Cristiano Poleto[2]

[1]Universidade Federal do Triângulo Mineiro, Uberaba, MG, Brazil
[2]Universidade Federal do Rio Grande do Sul, Porto Alegre, RS, Brazil
E-mails: patricia_ambiental@hotmail.com (PDM), cristiano.poleto@ufrgs.br (CP)

Received: May 13, 2016 - Revised: September 22, 2016 - Accepted: November 27, 2016

ABSTRACT

The concern with water quality has been promoting development of better monitoring and control techniques every day. As sediments transport most of water contaminants, their study is fundamental. Given the large number of variables for estimating sediment concentration and high costs of monitoring campaigns, it becomes necessary to develop more accessible methods which bring satisfactory practical results. Therefore, this work deals with application of the principle of maximum entropy, a probabilistic method to determine concentration of sediments in river channels with various concentrations and particle sizes. For this purpose, it was proposed a relationship between the theory of entropy parameters in order to reduce the computational effort. The results were satisfactory at concentrations above 10 g/L with R^2 greater than 0.88. The calculated squared errors in this study were lower than those found when using the theory of entropy by Tsallis and the equation of Rouse, classic models for determining the sediment concentration profile. The applicability of the proposed model and the ease of using the probabilistic method, since it reduces the amount of data needed to perform the estimate, makes it feasible on a global scale.

Keywords: Sedimentology; Water resources; Modeling.

RESUMO

A preocupação com a qualidade das águas vem promovendo o desenvolvimento de técnicas cada dia melhores de monitoramento e controle. Como os sedimentos transportam a maior parte dos contaminantes da água, seu estudo é fundamental. Diante do elevado número de variáveis existentes para a estimativa da concentração de sedimentos e elevados custos de campanhas de monitoramento, torna-se necessário o desenvolvimento de métodos mais acessíveis e que tragam resultados práticos satisfatórios. Para tanto, este trabalho trata da aplicação do princípio da entropia máxima, um método probabilístico, para determinar a concentração de sedimentos em calhas com diversas concentrações e granulometrias. Para isso, foi proposta uma relação entre os parâmetros do princípio da entropia máxima para determinar o índice entrópico e facilitar o cálculo. Os resultados mostraram-se satisfatórios para concentrações acima de 10 g/L com R^2 superiores a 0,88. Os erros quadráticos calculados neste trabalho foram inferiores aos encontrados quando utilizada a teoria da entropia por Tsallis e pela Equação de Rouse, modelos clássicos de estimativa do perfil de concentração de sedimentos. A aplicabilidade do modelo proposto e a facilidade da utilização do método probabilístico, já que reduz a quantidade de dados necessários para realizar a estimativa, torna-o viável em escala global.

Palavras-chave: Sedimentologia; Recursos hídricos; Modelagem.

INTRODUCTION

Concern about water resources is now a reality. It is known that the amount of water is not changed on the planet, but its distribution and quality make it impossible to use. Poleto et al. (2009) state that most of water contamination is due to sediments, especially the fine sediments that are transported to distant areas. In urban areas this effect is greater due to large diffuse pollution.

In order to identify and solve this problem, programs for monitoring the quantity and quality of sediment should be made feasible in an integrated water resources management system. However, resources are limited to serve the entire national territory. It is necessary to use more accessible techniques which bring satisfactory practical results.

The knowledge of the sediment transport rate is necessary for a number of purposes such as control and management of watersheds, river channels, sedimentation in reservoirs and transport of pollutants. To determine this, it is necessary to find the average sediment concentration in a section of the channel (CUI; SINGH, 2014).

Solid discharge measurement can be done by direct and indirect methods and is divided into solid discharge measurement in suspension, responsible in most cases for about 90% of the total discharge, and by the measurement of solid drag discharge, remaining with the rest of the percentage (CARVALHO, 2008).

Suspended solid discharge is the measure of transport of suspended sediment. The sediment distribution in a river section is not uniform. According to Vanoni (1977), the forces acting on the sediment particle are a function of particle size (granulometry), flow regime (laminar or turbulent), stream velocity, bed obstacles, water temperature, and so forth. Then, for the same composition of bottom sediments, particles drag, roll or move by salting if velocity is low, and as velocity increases, some of that sediment is carried to a zone where the flow is larger, turning into suspended sediment. The rest remains in the deepest layer of the water body (CARVALHO, 2008; SOS, 1963; WMO, 1981).

The sediment in suspension is subject to the action of flow velocity in the horizontal direction, predominantly, and its weight (ONGLEY, 1996; MERTEN et al., 2014). For this reason, the sediment concentration has a minimum on the surface and a maximum near the bed, for a varied granulometry. Sand particles are coarser sediments and present an increasing surface variation for the bed. The finer ones, such as silt and clay, have an approximately uniform distribution (SOS, 1963). For this reason, the measurement at one point does not represent the concentration of the section. It is necessary to perform sampling along the section, punctual or vertical, in a number suitable for the characterization of the section.

An important consideration to be made is that direct measurements in rivers are instantaneous measurements, because when it comes to flow measurement and sediment concentration, when collecting water at one point, the next will not be at the same time. Unless all water from the section is collected at a given time, the measurement of sediment discharge in rivers is always by sampling.

In current operations, the average sediment concentration of the section of a channel is determined with the ratio of the representative sediment concentration to the average sediment concentration of a vertical section line. This is a common practice in sampling the average depth to directly determine the mean vertical concentration.

However, during floods and periods of unstable flow, where sediment transport is significant, strong currents make sampling of the average depth unfeasible. As an alternative to this situation, models that translate the average concentration into a single sample are used.

Mathematical models are developed to describe the distribution of sediment concentration from the bed to the surface of the water in channels. These models can be used to estimate the average sediment concentration quickly using point samples in rivers. Simons and Sentürk (1992) attribute to O'Brien-Chistiansen the first deterministic turbulent diffusion equation for the non-uniform sediment distribution, derived from the continuity equation that can be used in two-dimensional uniform turbulent flow.

A classic example of a deterministic method is the Rouse equation (ROUSE, 1937). Several combinations of this equation are derived for estimating sediment concentration.

Einstein (1950) was the first to present a proposal for the study of sediment transport based on the probabilistic concept in the description of the movement of solid particles. The theoretical model devised by Einstein is based on the intense exchange between the particles that are in movement and those that are at rest. This model expresses the equilibrium condition between these exchanges. From this, other researchers began to use the concept of probability in their studies. According to Paiva (2007), the most relevant ones were: Brown (1950) Einstein and Barbarossa (1952), Colby and Hembree (1955), Toffaleti (1969). The work of Toffaleti (1969) is based on the Einstein method and allows the separate calculation of suspended and trailing sediments.

According to Chiu et al. (2000), models can be produced with the combination of deterministic and probabilistic concepts. The complementary feature of the two concepts strengthens the method and better describes sediment transport characteristics.

Cui and Singh (2014) compared the estimation of sediment discharge by the Tsallis entropy theory with the Prandtl von Karman methods and the Rouse equation, and verified that the methods based on the entropy of both Tsallis and Shannon presented better results.

Therefore, the principle of the maximum entropy by Tsallis is used to estimate the sediment concentration profile. However, one disadvantage of using the entropy is in the high number of unknowns, 3 unknowns and only 2 equations, making it an underdetermined system in which there are infinite solutions. Due to complexity of equations, a relation was proposed between two parameters, in this way, the number of unknowns was reduced and the numerical solution became possible. The alternative formulation allows the use of 3 points of measurements in the field, maximum and minimum concentration, and any point in the vertical to estimate the average sediment concentration. This facilitates estimation of sediment concentration and reduces field sampling time.

Thus, the main objective of the work is to apply an alternative formulation to determine the entropic index m and compare the results with those found in works of Einstein and Chien (1955) and Coleman (1981). The results were satisfactory for concentrations above 10 g/L in all studied profiles, regardless of granulometry and flow conditions.

Entropy theory

In 1824, the French physicist Carnot envisioned the Second Law of Thermodynamics in his studies on the flow of energy. By 1877, the Austrian Ludwig Boltzmann for the first time introduced the statistical concept of entropy, establishing a direct relationship between entropy and molecular disorder of a random thermal process, according to Resnick (2008).

Recently, Capek and Sheehan (2004) presented 21 formulations of entropy that can be divided into 5 categories according to the application: 1) devices and process impossibilities; 2) motors; 3) balance; 4) entropy; or 5) mathematical sets and spaces.

In general, it can be said that the entropy is a variable that reflects the state in which a thermodynamic system can be found. (CHIU, 1987; CONTE, 2005; CUI; SINGH, 2014; KUMBHAKAR; GHOSHAL, 2016; SINGH, 2011; YEVJEVICH, 1972).

Conte (2005) identifies a certain physical similarity between a hydraulic and a thermal system. The author compares these two systems as if they were two reservoirs that are disconnected at first: one is hot and the other is cold in the thermal reservoirs or one is full and the other is empty in the hydraulic reservoirs. After providing a communication between the two reservoirs, hot-cold or full-empty, it will take some time to establish the equilibrium condition of these reservoirs. In the final state, the two thermal reservoirs will have an average temperature and the two hydraulic reservoirs will be level. In both cases, the physical concept of entropy is present, according to the Second Law of Thermodynamics, the two systems, irreversibly, will never return spontaneously to their original state, unless a certain amount of energy is expended to perform such an operation. In the hydraulic reservoir, the energy that causes the water to move is the gravitational potential. In thermodynamic systems, it was necessary to introduce the concept of an "invisible" variable that was called entropy, to represent the flow of something moving from one reservoir to the other. In this way, Minei (1999) points out that the Second Law of Thermodynamics consists of the description of the spontaneous change of the energy distribution, from the unequal to the balanced one. According to Minei (1999), Clausius in 1950 suggested that this process of leveling applied to all forms of energy and to all events in the Universe.

In an isolated system, the entropy always grows. Since it is a probabilistic process, it is valid only for systems composed of a very large number of particles moving chaotically, according to the law of large numbers in probability theory (MINEI, 1999).

A system is characterized by its macroscopic variables, which are those quantities that can be measured in the laboratory: volume, pressure, temperature, total energy, chemical constitution. These quantities, however, are not sufficient to fully define the state of the system. There are a huge number of "microscopic variables" that are difficult to determine: the position and velocity of each individual particle, the quantum state of atoms or molecular structure, etc. For a "macroscopic state", there is a very large but finite number of possible "microscopic states" defined by the distribution of particles, atoms or molecules, in space or by distribution of energy between them. Due to the chaotic movement and the constant shocks between them, there is a certain "microscopic state" or "complexion" at each moment. As no state has preponderance over the others, there is a continual change of "microscopic states." The number of "microscopic states" satisfying a given "macroscopic state" is called the thermodynamic probability of the state, the statistical weight of the state, or the number of complexions. Unlike mathematical probability, which always has the value of a function of its own, the value of P is always expressed by an integer, usually very large. If a spontaneous transformation occurs in an isolated system which, as a consequence, changes the "macroscopic state" of the system, this means that the new state has a greater amount of "microscopic states" or "complexions" satisfying it than the previous one. As a result, it increases the thermodynamic probability of the system and, simultaneously, the entropy of the system (MINEI, 1999, p. 13).

Thus, Capek and Sheehan (2004) state that entropy is a macroscopic quantitative measure of microscopic disorder.

The statistical concept of entropy has evolved. In 1948, Shannon proposed a theory with more solid mathematical bases, establishing a connection between entropy and typical sequences that allowed the solution of numerous problems in the areas of coding and transmission of data in the communication systems in general. Considering the example of Hancock (1961), a student randomly flips through a book and stops, casually, in the chapter Discrete Probability. If he already knew the subject, he will get little or no information from the reading. If this is your first contact with the topic, he will be receiving a lot of information in that reading.

Thus, what differentiates the first situation from the second is the notion of uncertainty, that is, the greater the uncertainty about the result of a message "state", the greater the amount of information associated with that result. If it is possible to predict the outcome of a post-message situation in advance, then certainly no information was passed by it. The measurement of post-message "state" information must be based on the probability of occurrence of this situation. Entropy, therefore, is a measure of information or degree of uncertainty about a given system (SHANNON, 1948). Shannon's entropy can be seen as a discrete form of the classical Boltzmann-Gibbs entropy (CAPEK; SHEEHAN, 2004).

If an event occurs and a message is transmitted to communicate it, the amount of information transmitted to the receiver is defined by Equation 1:

$$\textit{Information Received} = \log\left(\frac{p'}{p}\right) \tag{1}$$

where: p' = probability of the event, next to the receiver, after the arrival of the message; p = probability of the event, next to the receiver, before the arrival of the message.

Assuming only the no-noise transmission situation, that is, the received message is the same as the transmitted message, the receiver is sure that it is receiving the correct message. Thus, the probability p' will be 1. The amount of information will depend only on the probability of the event prior to the message, so Equation 1 can be defined by Equation 2:

$$\textit{Information Received} = \log\left(\frac{1}{p}\right) = -\log p \tag{2}$$

There are other definitions that do not involve the logarithm, but the definition of Equation 2 is simple, since it does not lead to contradictions and has useful properties in the analysis (MINEI, 1999). According to the same author, the numerical value of the amount of information depends on the base used for the logarithms. In the transmission of information, normal is the base 2. Thus, an information unit is called a binary digit, usually called bit (SHANNON, 1948). In a situation where there are only two equally likely alternatives, a bit of information will tell which event occurred. Minei (1999) exemplifies this as in the launching of a coin. There are two alternatives, heads or tails, with equal probabilities. The result "tails" provides the specific amount of information according to Equation 3:

$$-\log_2\left(\frac{1}{2}\right) = \log_2(2) = 1\ bit \quad (3)$$

Considering a source producing 3 symbols, A, B and C, "A" occurs with probability P(A), "B" with probability P(B) and "C" with probability P(C). The amount of information associated with "A" is $-\log_2 P(A)$, the one associated with "B" is $-\log_2 P(B)$ and the one associated with "C" is $-\log_2 P(C)$. "A" occurs in time only with the probability P(A), "B" only with P(B) and C, only with P(C), and the average information H is defined by Equation 4:

$$H = -P(A)\log_2 P(A) - P(B)\log_2 P(B) - P(C)\log_2 P(C) \quad (4)$$

The concept of entropy is already well established and used in statistics and information theory. Generalizing the result in Equation 4 for an X source and generating m independent symbols, if the j[th] symbol has a probability of occurrence p (X_j), the entropy can be quantified in terms of probability according to Equation 5:

$$H(X) = -\sum p(X_j)\ log\, p(X_j) \quad (5)$$

where: $p(X_j)$ = the probability of the system being in state X with values of {Xj, j = 1, 2, ...}.

This has been shown in ideal systems, H(X) defined by Equation 5 is equivalent to the entropy of thermodynamics.

The entropy by Tsallis is a generalization of the Boltzmann-Gibbs and Shanoon entropy (CAPEK; SHEEHAN, 2004; CUI, 2011). The main advantage of Tsallis entropy is mathematical simplicity. It has been applied to numerous different physical phenomena which are considered beyond the reach of equilibrium thermodynamics. Notably, these include non-extensive long range systems, e.g., gravitational, electrostatic, such as plasmas and multiparticles, self-gravitating systems such as galaxies and globular clusters. It was applied to self-organizing behaviors and to chaotic systems such as financial markets, traffic, locomotion of microorganisms, subatomic particle collisions, and tornadoes. Unfortunately, its underlying physical base was not well established, prompting critics to label it as just a "curve fit." Its simplicity and adaptability, however, cannot be denied (CAPEK; SHEEHAN, 2004).

According to the concept of entropy, under conditions of static equilibrium, the system tends to have the maximum entropy over current constraints (CONTE, 2005).

However, the entropy H defined by Equation 5 is the average information content of a data sample. If the variable X is continuous, the entropy can be expressed by Equation 6:

$$H(X) = -\int p(X)\ln p(X)dX \quad (6)$$

where $p(X)$ is the probability density function so that $p(X)dX$ is the probability of the variable being between X and X+dX.

The maximum entropy is related to the amount of information about a variable X, which is equivalent to the maximum uncertainty of X so far measured.

The principle of maximum uncertainty reveals that the maximum entropy is a function of the number of possibilities N that this system can find. For example, the act of playing a 6-sided die. The maximum entropy of this system is ln6, since the probability of a given face facing upwards is the same for all faces. It can be said that the entropy decreases as information about the system increases or vice versa (CONTE, 2005).

It is 0 in purely deterministic cases in which the joint probability function $p(X_j) = 1$ and (Xi) = 0 for every i other than j. Maximizing the system entropy will make uniform probability distribution possible as long as it meets the constraints.

According to Minei (1999), the lower the entropy, the more unequal the energy distribution. The greater the entropy, the more balanced the distribution. In this way, the maximum entropy has the equilibrium state of a system. The spontaneous tendency is in the sense of balancing unequal distributions of energy, so everything moves in the direction of a low to a high entropy.

According to the concept of entropy, it is possible, by maximum entropy, to determine the maximum uncertainty, randomness or disorder of a system. Considering a hydrological system, the principle of maximum entropy is used to model the probability distribution of the possible state of the system. The data can be collected for parameter estimation and later validation (KUMBHAKAR; GHOSHAL, 2016).

Application of entropy in hydrology and hydraulics

In general, in the traditional approach to hydraulics, the quantities involved are treated in a deterministic manner. In fact, these quantities, represented by an average value, are sample means and should be presented statistically by a mean and a variance, considering the uncertainty of any sample mean (MINEI, 1999).

The concept of entropy as used in Information Theory provides the degree of uncertainty of a particular result in a process; therefore, for the treatment of hydrological variables, one can calculate the entropy of these variables from historical and/or measured data and thus characterize the unexpected or the inherent variability of the process (CHIU, 1987; ESPILDORA; AMOROCHO, 1973; SINGH, 1989). Several works have been developed applying the theory of entropy. In the area of water resources (SINGH, 1997; HUSAIN, 1989), in the application in hydrology (WANG; ZHU, 2001; SINGH, 1998), in historical series of precipitation and flow, mainly. In the prediction of hydrological variables (CONTE, 2005; WEIJS et al., 2010), in the evaluation of the prediction and stability of river flows (MUKHOPADHYAY; KHAN, 2015), in the estimation of the sediment concentration

(SINGH; CUI, 2015; CUI; SINGH, 2014; GAN et al., 2014; LIEN; TSAI, 2003; CHIU et al., 2000; LUO; SINGH, 2011; GOMEZ; PHILLIPS, 1999; SING et al., 1988; CHIU, 1988; CHAO-LIN CHIU, 1987; SINGH; KRSTANOVIC, 1987), in the estimation of the precipitation ratio X flow (SINGH, 2012; CONTE, 2005; SONUGA, 1976), in river processes (XU; ZHAO, 2013; DESHPANDE; KUMAR, 2013), among other applications.

The velocity distribution equation derived from the principle of maximum entropy has advantages over the universal equation of velocity distribution of Prandtl-von Karman. The maximum entropy applied to the velocity distribution and sediment transport reflects the effect of particle size of suspended sediment, coarse material and sediment concentration. They can be used as variables to characterize and compare various flows (SINGH; CUI, 2015; CHAO-LIN CHIU, 1987).

Chiu et al. (2005) and Minei (1999) established river flow estimation methods using the probabilistic model based on the Shannon entropy with the velocity measurement at only one point of a vertical of the river or some points of that river vertical. This greatly reduces the time and cost of sampling. In addition, it makes possible the measuring during floods when the water level undergoes large variations in a short time. This technique can be applied when using radars on the surface of water and even ADCPs (Acoustic Doppler Current Profiler), especially during floods. The surface velocity is measured and then it is possible to find the entropy parameters. The channel section is calculated by calculating the discharge or total flow (MORIASI et al., 2007). The discharge data obtained by such methods can also be used to understand the ratios of the discharge phases occurring during unstable high flow periods, which have the forms different from those presented by the conventional classification curves obtained with constant flow periods (CHIU et al., 2005). Such advances should add scientific knowledge to hydrology and may also contribute greatly to engineering projects for flood control. Once the channel section is known, the discharge or total flow is calculated (CHIU et al., 2005; MORAMARCO et al., 2013). The discharge data obtained by such methods can also be used to understand the ratios of the discharge phases occurring during unstable high flow periods, which have the forms different from those presented by the conventional classification curves obtained with constant flow periods (CHIU et al., 2005). Such advances should add scientific knowledge to hydrology and may also contribute greatly to engineering projects for flood control.

MATERIAL AND METHODS

To determine the sediment concentration in different flow regimes and grain sizes, two data series were collected by Coleman (1981) and Einstein and Chien (1955). These two data series were used because of their significance in sediment transport studies and because they present the greatest detail of the sediment concentration profile. These two aspects are important for the validation of the proposed method.

For this, the conditions of accomplishment of each one of the works under different conditions of flow and granulometry will be detailed.

The Coleman (1981) experiment was performed on a rectangular channel 0.356 m wide and 15 m long with an adjustable slope to maintain the flow. The particle size (D), discharge (Q) and velocity (U*) of each profile are shown in Table 1.

On the other hand, the Einstein and Chien (1955) experiment was performed on a 0.31 m wide, 0.36 m deep, and 12.19 m long channel. The slope was adjusted through a connector ranging from 0.0185 to 0.025, and the discharge ranged from 0.074 to 0.085 m^3/s. The water depth (H), the mean velocity (U*) and the diameter at which 50% of the material is retained (D_{50}) can be seen in Table 2.

Three different types of sand were used in their experiments of Einstein and Chien (1955), which were evaluated as coarse, with D50 of 1.3 mm, medium with D50 of 0.94 mm and fine with D50 of 0.274 mm.

Table 1. Conditions of the Coleman (1981) experiment.

Profile	D	Q	U*
	mm	m^3/s	m/s
Coleman1	0.105	0.064	0.041
Coleman2	0.105	0.064	0.041
Coleman3	0.105	0.064	0.041
Coleman4	0.105	0.064	0.041
Coleman5	0.105	0.064	0.041
Coleman6	0.105	0.064	0.041
Coleman7	0.105	0.064	0.041
Coleman8	0.105	0.064	0.041
Coleman9	0.105	0.064	0.041
Coleman10	0.105	0.064	0.041
Coleman11	0.105	0.064	0.041
Coleman12	0.105	0.064	0.041
Coleman13	0.105	0.064	0.041
Coleman14	0.105	0.064	0.041
Coleman15	0.105	0.064	0.041
Coleman16	0.105	0.064	0.041
Coleman17	0.105	0.064	0.041
Coleman18	0.105	0.064	0.041
Coleman19	0.105	0.064	0.041
Coleman21	0.210	0.064	0.041
Coleman22	0.210	0.064	0.041
Coleman23	0.210	0.064	0.041
Coleman24	0.210	0.064	0.041
Coleman25	0.210	0.064	0.041
Coleman26	0.210	0.064	0.041
Coleman27	0.210	0.064	0.041
Coleman28	0.210	0.064	0.041
Coleman29	0.210	0.064	0.040
Coleman30	0.210	0.064	0.041
Coleman31	0.210	0.064	0.041
Coleman32	0.420	0.064	0.041
Coleman33	0.420	0.064	0.041
Coleman34	0.420	0.064	0.041
Coleman35	0.420	0.064	0.041
Coleman36	0.420	0.064	0.041
Coleman37	0.420	0.064	0.041
Coleman38	0.420	0.064	0.043
Coleman39	0.420	0.064	0.044
Coleman40	0.420	0.064	0.045

U* = the shear velocity. D = diameter of the particles. Q = flow.

Table 2. Conditions of the Einstein and Chien (1955) experiment.

Profile	H	U*	D_{50}
	mm	m/s	mm
RunS1	138	0.115	1.3
RunS2	120	0.129	1.3
RunS3	120	0.133	1.3
RunS4	115	0.144	1.3
RunS5	109	0.144	1.3
RunS6	142	0.118	0.94
RunS7	142	0.118	0.94
RunS8	139	0.115	0.94
RunS9	135	0.118	0.94
RunS10	128	0.125	0.94
RunS11	133	0.0767	0.274
RunS12	132	0.0767	0.274
RunS13	134	0.0767	0.274
RunS14	124	0.0767	0.274
RunS15	124	0.0767	0.274
RunS16	119	0.0767	0.274

H= water depth. U*= mean velocity or shear velocity. D50 = diameter at which 50% of the material is retained.

The flow conditions and granulometry of each of the profiles (S) of Einstein and Chien (1955) can be visualized in Table 2.

Method for the estimation of sediment concentration

The estimation of the sediment concentration using the Tsallis entropy implies in (1) definition of Tsallis entropy, (2) specification of restrictions, (3) maximization of entropy, (4) determination of Lagrange multipliers, (5) determination of the probability density function and maximum entropy, (6) hypothesis of cumulative probability distribution, and (7) sediment concentration distribution. These steps were detailed by (CUI; SINGH, 2014) and are described below. After these steps, changes in sediment concentration distribution were performed to reduce the number of parameters and to facilitate calculations (8).

Definition of the Tsallis entropy

Given that the concentration of sediments "c" is a random variable with function of density and probability, f(c), then the Tsallis entropy (TSALLIS, 1988) of "c", H(c), can be expressed by Equation 7:

$$H(c)=\frac{1}{m-1}\left\{1-\int_{Ch}^{Cm}\left[f(c)\right]^{m}dc\right\}=\frac{1}{m-1}\int_{Ch}^{Cm}f(c)\left\{1--\left[f(c)\right]^{m-1}\right\}dc \quad (7)$$

where c, $c_h \le c \le c_m$, is the value of the random variable c, c_m is the maximum value of "c" or bed concentration, c_h is the concentration on the water surface, the symbol m represents the entropy index, and H represents the entropy of f(c) or "c" (CHIU; JIN, 1997).

When m = 1, the entropy by Tsallis is equal to that of Boltzmann-Gibbs and Shanoon (CAPEK; SHEEHAN, 2004; CUI, 2011). The entropic index, non-extensivity parameter m, is considered a measure of the fractal nature of the path of a system in phase space. It is able to show the rapid and radical changes in behavior and phase (CAPEK; SHEEHAN, 2004).

Specification of restrictions

The f(c) is a Probability Density Function and must satisfy Equation 8:

$$\int_{c_h}^{c_m}f(c)\,dc=1 \quad (8)$$

One of the simplest constraints is the mean or equilibrium sediment concentration by volume, called cD. The mean value may be known or obtained from observations, and can be expressed by Equation 9:

$$\int_{c_h}^{c_m}cf(c)\,dc=E[c]=c_D \quad (9)$$

Entropy maximization

The entropy H of c, given by Equation 7 can be maximized, according to Jaynes (1957), using the Lagrange multiplier method. For this purpose, the Lagrange function L can be expressed by Equation 10:

$$L=\int_{c_h}^{c_m}\frac{f(c)}{m-1}\left\{1-\left[f(c)\right]^{m-1}\right\}dc-\lambda_0\left[\int_{c_h}^{c_m}f(c)dc-1\right]--\lambda_1\left[\int_{c_h}^{c_m}cf(c)dc-c_D\right] \quad (10)$$

where λ_0 and λ_1 are the Lagrange multipliers. Differentiating Equation 10 with respect to f, highlighting f as a variable and "c" as a parameter, and equating the derivative to zero, it is obtained:

$$\frac{\partial L}{\partial f}=0\rightarrow\frac{1}{m-1}\left[1-mf(c)^{m-1}\right]-\lambda_0-\lambda_1=0 \quad (11)$$

Equation 11 leads to Equation 12

$$f(c)=\left[\frac{m-1}{m}\left(\frac{1}{m-1}-\lambda_0-\lambda_1 c\right)^{\frac{1}{m-1}}\right] \quad (12)$$

which represents the less biased density and probability function of sediment concentration "c" based on Jaynes (1957).

Determination of Lagrange multipliers

Equation 12 has unknown λ_0 and λ_1 that can be determined using Equations 8 and 9. The Lagrange multiplier λ_1 is associated with the mean concentration and λ_0 with the total probability. These multipliers have opposite signals, with λ_1 positive and λ_0 negative. The substitution of Equation 12 in Equation 8 leads to:

$$\int_{c_h}^{c_m}\left[\frac{m-1}{m}\left(\frac{1}{m-1}-\lambda_0-\lambda_1 c\right)^{\frac{1}{m-1}}\right]dc=1 \quad (13)$$

The integration of Equation 13 will be:

$$\frac{1}{\lambda_1}\left(\frac{m-1}{m}\right)^{\frac{m}{m-1}}\left[\left(\frac{1}{m-1}-\lambda_0-\lambda_1 c_m\right)^{\frac{m}{m-1}}-\left(\frac{1}{m-1}-\lambda_0--\lambda_1 c_h\right)^{\frac{m}{m-1}}\right]=1 \quad (14)$$

Likewise, the substitution of Equation 12 in Equation 9 will be:

$$\int_{c_h}^{c_m} c\left[\frac{m-1}{m}\left(\frac{1}{m-1}-\lambda_0-\lambda_1 c\right)^{\frac{1}{m-1}}\right]dc = c_D \qquad (15)$$

Equation 15 can be integrated by parts such as:

$$-\lambda_1 c_D\left(\frac{m}{m-1}\right)^{\frac{m}{m-1}} = c_m\left(\frac{1}{m-1}-\lambda_0-\lambda_1 c_m\right)^{\frac{m}{m-1}} -$$

$$-c_h\left(\frac{1}{m-1}-\lambda_0-\lambda_1 c_h\right)^{\frac{m}{m-1}} + \frac{m-1}{2m-1}\frac{1}{\lambda_1} \qquad (16)$$

$$\left[\left(\frac{1}{m-1}-\lambda_0--\lambda_1 c_m\right)^{\frac{2m-1}{m-1}} - \left(\frac{1}{m-1}-\lambda_0-\lambda_1 c_h\right)^{\frac{2m-1}{m-1}}\right]$$

Equations 14 and 16 can be solved numerically for λ_0 and λ_1 for specified values of c, c_m, c_h, and m.

Determination of the Cumulative Distribution Function (CDF) and maximum entropy

Integrating Equation 12 from c_h to c yields the Cumulative Distribution Function of c, F(c), according to:

$$F(c) = \left(\frac{m-1}{m}\right)^{\frac{m}{m-1}}\frac{1}{\lambda_1}\left[\left(\frac{1}{m-1}-\lambda_0-\lambda_1 c_h\right)^{\frac{m}{m-1}} - \left(\frac{1}{m-1}-\lambda_0--\lambda_1 c\right)^{\frac{m}{m-1}}\right] \qquad (17a)$$

If the flow of sediments on the water surface is insignificant, that is, $c_h = 0$, then Equation 17a becomes:

$$F(c) = \left(\frac{m-1}{m}\right)^{\frac{m}{m-1}}\frac{1}{\lambda_1}\left[\left(\frac{1}{m-1}-\lambda_0\right)^{\frac{m}{m-1}} - \left(\frac{1}{m-1}-\lambda_0--\lambda_1 c\right)^{\frac{m}{m-1}}\right] \qquad (17b)$$

Now, the maximum entropy of c is obtained by inserting Equation 17b into Equation 7:

$$H(c) = \frac{1}{m-1}\left\{\begin{matrix} c_m - c_h + \left(\frac{m-1}{m}\right)^{\frac{m}{m-1}} + + \frac{1}{(2m-1)\lambda_1} \\ \left[\left(\frac{1}{m-1}-\lambda_0-\lambda_1 c_m\right)^{\frac{2m-1}{m-1}} - \left(\frac{1}{m-1}-\lambda_0--\lambda_1 c_h\right)^{\frac{2m-1}{m-1}}\right]\end{matrix}\right\} \qquad (18)$$

Equation 18 is expressed in terms of λ_0 and λ_1, Lagrange multipliers, by the lower limit of concentration, c_h, and upper limit of concentration c_m.

Cumulative Distribution Function (CDF)

The cumulative distribution function of "c", F(c), in terms of flow depth can be written as:

$$F(c) = \frac{h_0 - y}{h_0} = 1 - \frac{y}{h_0} \qquad (19)$$

Equating Equation 19 with Equation 17a, it becomes:

$$F(c) = \left(\frac{m-1}{m}\right)^{\frac{m}{m-1}}\frac{1}{\lambda_1}\left[\left(\frac{1}{m-1}-\lambda_0-\lambda_1 c_h\right)^{\frac{m}{m-1}} - \left(\frac{1}{m-1}-\lambda_0--\lambda_1 c\right)^{\frac{m}{m-1}}\right] = 1 - \frac{y}{h_0} \qquad (20)$$

Distribution of sediment concentration

For simplicity, considering $\lambda_* = \frac{1}{m-1} - \lambda_1$, then Equation 20 can be written as:

$$c = \frac{\lambda_*}{\lambda_1} - \frac{1}{\lambda_1}\frac{m}{m-1}\left\{-\lambda_1\frac{m-1}{m}\left(1-\frac{y}{h_0}\right) + \left[\frac{m-1}{m}\left(\lambda_* --\lambda_1 c_h\right)\right]^{\frac{m}{m-1}}\right\}^{\frac{m-1}{m}} \qquad (21)$$

If $c_h = 0$, Equation 21 reduces to:

$$c = \frac{\lambda_*}{\lambda_1} - \frac{1}{\lambda_1}\frac{m}{m-1}\left\{-\lambda_1\frac{m-1}{m}\left(1-\frac{y}{h_0}\right) + \left(\frac{m-1}{m}\lambda_*\right)^{\frac{m}{m-1}}\right\}^{\frac{m-1}{m}} \qquad (22)$$

Equation 22 represents the defined sediment concentration distribution in terms of flow depth.

Reparametrization

The distribution of sediment concentration can be simplified using a dimensionless entropy parameter defined as:

$$\mu = \frac{\lambda_1 c_m}{\lambda_1 c_m - \lambda_*} - \frac{1}{\lambda_1}\frac{m}{m-1} \qquad (23)$$

Dividing Equation 22 by c_m, we obtain:

$$\frac{c}{c_m} = \frac{\lambda_*}{\lambda_1 c_m} - \frac{1}{\lambda_1 c_m}\frac{m}{m-1}\left\{-\lambda_1\frac{m-1}{m}\left(1-\frac{y}{h_0}\right) + \left(\frac{m-1}{m}\lambda_*\right)^{\frac{m}{m-1}}\right\}^{\frac{m-1}{m}} \qquad (24)$$

Since $\frac{\lambda_*}{\lambda_1 c_m} = 1 - \frac{1}{\mu}$, μ from Equation 23, Equation 24 can be reformulated as:

$$\frac{c}{c_m} = 1 - \frac{1}{\mu}\left\{1 - \left[\left(\frac{m}{m-1}\right)^{\frac{m}{m-1}}\frac{\mu}{c_m}\left(-\frac{y}{h_0}\right) + 1\right]^{\frac{m-1}{m}}\right\} \qquad (25)$$

If $c_h = 0$ at $y = h_0$, Equation 25 reduces to:

$$0 = 1 - \frac{1}{\mu}\left\{1 - \left[1 - \left(\frac{m}{m-1}\right)^{\frac{m}{m-1}}\frac{\mu}{c_m}\right]^{\frac{m-1}{m}}\right\} \qquad (26)$$

Equation 26 suggests:

$$\left(\frac{m}{m-1}\right)^{\frac{m}{m-1}}\frac{\mu}{c_m} = 1 - (1-\mu)^{\frac{m}{m-1}} \qquad (27)$$

Substituting Equation 27 into Equation 25, the distribution of the dimensionless sediment concentration with $c_h = 0$ becomes:

$$\frac{c}{c_m} = 1 - \frac{1}{\mu}\left(1 - \left\{(1-\mu)^{\frac{m}{m-1}} + \left[1 - (1-\mu)^{\frac{m}{m-1}}\right]\left(1 - -\frac{y}{h_0}\right)\right\}^{\frac{m-1}{m}}\right) \quad (28)$$

Equation 28 expresses the sediment concentration distribution as a function of the vertical distance y.

Reduction of parameters

In order to estimate the sediment concentration distribution in a given section, it was used the probabilistic model of Cui and Singh (2014), which can be visualized in Figure 1, expressed by Equation 29:

$$c = \frac{\lambda_*}{\lambda_1} + \frac{1}{\lambda_1}\frac{m}{m-1}\left\{-\lambda_1\frac{m-1}{m}\left(1 - \frac{y}{h_0}\right)^a + \left[\frac{m-1}{m}(\lambda_* + +\lambda_1 c_h)\right]^{\frac{m}{m-1}}\right\}^{\frac{m-1}{m}} \quad (29)$$

Since $\lambda_* = \frac{1}{m-1} - \lambda_1$ where:
c = concentration of sediments at a vertical distance y, dimensionless; c_m = maximum value of C or concentration in the bed, dimensionless; c_h = concentration on the water surface, dimensionless; m = entropy parameter, dimensionless; λ_1 = Lagrange multiplier, dimensionless; h_0 = depth of flow, in meters; a = parameter related to the characteristics of sediment particles.

Equation 29 differs from Equation 22 by the introduction of parameter "a" which is related to particle characteristics such as size, roughness, among others (CUI; SINGH, 2014).

Equation 29 can be rewritten to any point (Equation 30) and to the one with the highest sediment concentration at the deepest point of the river (Equation 31).

$$c = \frac{\lambda_*}{\lambda_1} + \frac{1}{\lambda_1}\frac{m}{m-1}\left\{-\lambda_1\frac{m-1}{m}\left(1 - \frac{y}{h_0}\right)^a + \left[\frac{m-1}{m}(\lambda_* + +\lambda_1 c_h)\right]^{\frac{m}{m-1}}\right\}^{\frac{m-1}{m}} \quad (30)$$

$$c_m = \frac{\lambda_*}{\lambda_1} + \frac{1}{\lambda_1}\frac{m}{m-1}\left\{-\lambda_1\frac{m-1}{m}(1)^a + \left[\frac{m-1}{m}(\lambda_* + \lambda_1 c_h)\right]^{\frac{m}{m-1}}\right\}^{\frac{m-1}{m}} \quad (31)$$

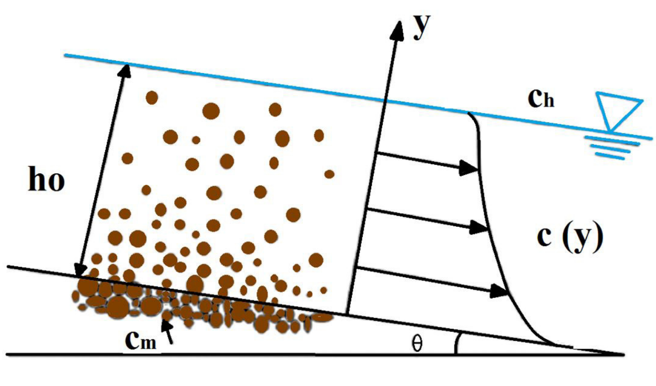

Figure 1. Uniform flow of sediments. Where c (y) = concentration of sediments at a vertical distance y, dimensionless; cm = maximum value of C or concentration in the bed, dimensionless; ch = concentration on the water surface, dimensionless; h0 = depth of flow, in meters; θ angle of inclination of the bed.

Reorganizing Equation 29 suggested by Cui and Singh (2014), we have:

$$\frac{1}{c_m} = \frac{1}{c}\left(\frac{\lambda_*}{\lambda_1 c_m} - \frac{1}{\lambda_1 c_h}\frac{m}{m-1}\left\{-\lambda_1\frac{m-1}{m}\left(1 - \frac{y}{h_0}\right)^a + \left[\frac{m-1}{m}(\lambda_* - -\lambda_1 c_h)\right]^{\frac{m}{m-1}}\right\}^{\frac{m-1}{m}}\right) \quad (32)$$

Inverting Equation 31 deduced in this work, it becomes:

$$\frac{1}{c_m} = \frac{\lambda_1}{1+\lambda_1}\left\{-\lambda_1\frac{m-1}{m}(1)^a + \left[\frac{m-1}{m}(\lambda_* - \lambda_1 c_h)\right]^{\frac{m}{m-1}}\right\}^{\frac{1-m}{m}} \quad (33)$$

Equating Equations 32 and 33:

$$\frac{1}{c}\left(\frac{\lambda_*}{\lambda_1 Cm} - \frac{1}{\lambda_1 Cm}\frac{m}{m-1}\left\{-\lambda_1\frac{m-1}{m}\left(1 - \frac{y}{h_0}\right)^a + \left[\frac{m-1}{m}(\lambda_* - -\lambda_1 c_h)\right]^{\frac{m}{m-1}}\right\}^{\frac{m-1}{m}}\right) =$$
$$\frac{\lambda_1(m-1)}{\lambda_1(m-1)-m}\left\{-\lambda_1\frac{m-1}{m}(1)^a + \left[\frac{m-1}{m}(\lambda_* - -\lambda_1 c_h)\right]^{\frac{m}{m-1}}\right\}^{\frac{1-m}{m}} \quad (34)$$

Simplifying the equality expressed in Equation 34, considering $T1 = -\lambda_1\frac{m-1}{m}\left(1 - \frac{y}{D}\right)^a + \left[\frac{m-1}{m}(\lambda_* + \lambda_1 c_h)\right]^{\frac{m}{m-1}}$, and $T2 = -\lambda_1\frac{m-1}{m}(1)^a + \left[\frac{m-1}{m}(\lambda_* + \lambda_1 c_h)\right]^{\frac{m}{m-1}}$, we have:

$$ln\left(\frac{(1+\lambda_1)^2}{\lambda_1(1+CCm)}\right) + \frac{m-1}{m}\ln(T1T2) = 0 \quad (35)$$

Therefore, we obtain a system with three unknowns: λ_1, a, $e\ m$ and two equations. The variables c_h, c and c_m, as well as y and h_0 must be obtained in the field data. In this work the relation of $m = \exp F(c)^{\lambda_1}$.

Equation 35 is the basis of the developed method. Unlike previous work, the minimum concentration is not considered as 0.

In the simulation, besides the relation $m = \exp F(c)^{\lambda_1}$ of m, it was adopted the function $a = a'^{((y/ho)*22)}$ For the parameter "a", where a' is a parameter to be measured, y is the depth of the point and ho is the maximum depth. As well as "m", a' is determined by the solution of the system detailed in the item "Reduction of parameters", presented in Equation 35, taking into consideration T1 and T2.

Validation

In order to evaluate efficiency of the model, the following statistical coefficients were applied: Nash-Sutcliffe efficiency (NSE); coefficient of determination (R^2); Deviation between observed and simulated flows (D%); Pbias; ratio of the root mean square error to the standard deviation of measured data (RSR); e root-mean-square error (RMSE). Subsequently, their formulations are presented, where c_{obs} and c_{calc} refer to the observed and calculated concentrations, respectively, in g/L.

According to Molnar (2011), the value of the Nash-Sutcliffe coefficient indicates the adjustment of the simulated data to those observed in the 1: 1 line, which can vary from -∞ to 1. Molnar

(2011) presented the following classification for this coefficient, using daily simulation step: NSE> 0.8 the model is considered excellent; 0.8 <NSE <0.6 the model is considered very good; 0.4 <NSE <0.6 the model is considered good, between 0.4 and 0.2, satisfactory and <0.2 insufficient. According to Moriasi et al. (2007), NSE values above 0.5 qualify the model for simulation.

$$NSE = 1 - \frac{\sum_{i=1}^{N}\left(c_{obsi} - c_{calci}\right)^2}{\sum_{i=1}^{N}\left(c_{obsi} - \overline{c_{obs}}\right)^2} \tag{36}$$

The R^2 value, according to Willmott et al. (1985), is an indicator of the correlation between observed and simulated values, with amplitude of variation between 0 and 1, where the value 1 indicates a perfect fit. This coefficient is considered one of the most sensitive statistics to extreme values. R2 values above 0.5 are considered as acceptable (Moriasi et al., 2007).

$$R^2 = \frac{\sum_{i=1}^{N}\left(c_{obsi} - \overline{c_{obs}}\right) * \left(c_{calci} - \overline{c_{calc}}\right)}{\left[\sum_{i=1}^{N}\left(c_{obsi} - \overline{c_{obs}}\right)^2\right]^{0.5} * \left[\sum_{i=1}^{N}\left(c_{calci} - \overline{c_{calc}}\right)^2\right]^{0.5}} \tag{37}$$

The value of D means the average trend of the estimates produced by the model and, when positive, expresses a tendency of overestimation and when negative, of underestimation. Liew et al. (2003) cited by Viola et al., (2012) present the following ranges and respective interpretations of D: <10%, very good; between 10% and 15%, good; between 15% and 25%, satisfactory and> 25%, the model produces inadequate estimates regarding the trend.

$$D(\%) = \frac{\sum_{i=1}^{N}\left(\frac{c_{calci} - c_{obsi}}{c_{obsi}}\right) * 100}{N} \tag{38}$$

Pbias also measures deviation of data. When positive, the model tends to overestimate the data and when negative, to underestimate the simulated data in relation to the measured ones. An ideal model would have a value of 0.

$$Pbias(\%) = \frac{\sum_{i=1}^{N}\left(c_{obsi} - c_{calci}\right) * 100}{\sum_{i=1}^{N}\left(c_{obsi}\right)} \tag{39}$$

RSR is the relation between the root mean square error to the standard deviation of measured data:

$$RSR = \frac{RMSE}{STDEV_{obs}} = \frac{\sqrt{\sum_{i=1}^{N}\left(c_{calci} - c_{obsi}\right)^2}}{\sqrt{\sum_{i=1}^{N}\left(c_{obsi} - c_{médio}\right)^2}} \tag{40}$$

The root-mean-square error allows to quantify the magnitude of the deviations of the simulated values in relation to the observed ones. The closer to 0, the better the data adjustment. It is expressed by:

$$RMSE = \sqrt{\frac{\sum_{i=1}^{N}\left(c_{calci} - c_{obsi}\right)^2}{N}} \tag{41}$$

Moriasi et al. (2007) reported intervals of values and performance evaluations for the recommended statistics and established guidelines for evaluation of flow simulation models, sediment transport and nutrients. Based on this analysis, they recommended three quantitative statistics: Nash-Sutcliffe efficiency (NSE), percent bias (Pbias) and ratio of the root mean square error to the standard deviation of measured data (RSR), besides the graphic techniques, to be used in the evaluation of models. In general, model simulation can be judged to be satisfactory if NSE> 0.50 and RSR <0.70, and if PBIA <= 55% for sediments.

RESULTS AND DISCUSSION

Using the relation of $m = \exp F(c)^{\lambda_1}$, it was possible to reduce the solution of sediment concentration profile estimation to 2 unknowns.

It is possible to note in Figure 2 the estimate made with the data of Coleman (1981). The profiles from 2 to 20 correspond to group 1, from 22 to 31 group 2 and 33 to 40 group 3. The data from group 1 have a granulometry of 0.105 mm, group 2 of 0.210 mm and group 3 of 0.420 mm. All Coleman data were simulated with a constant flow of 0.064 m^3/s. Concentrations were minimal in the first experiments of each group increasing until the last. Profiles 1, 21 and 32 had the concentration 0 and are not mentioned. Profiles 20, 31 and 40 had the highest concentrations.

It can be observed (Figure 2) that the model is better suited to profiles with high concentrations. Profiles 2, 3, 22 and 23 and all profiles of Group 3 show differences between the measured and estimated values at the surface.

It can be seen from the D% value that the model overestimated the concentrations below 5 g/L of the profiles 2 to 6 of Group 1 and 22 to 27 of Group 2 as can be proved by the D% value (see Table 3). It also overestimated the concentrations below 10 g/L with a grain size of 0.420 mm from the Group's 33-40 profiles. Although profiles 2, 22, 33, 34 and 35 showed unsatisfactory results for NSE, all other profiles presented satisfactory results for R^2.

Taking into account that the Pbias limit for sediments is 55%, the measured data had values smaller than those observed only in profiles 2, 33, 34, 35 and 36. Therefore, by Pbias, there was no overestimation of the profiles 3.4, 5.6, 22, 23, 24.25, 26, 27.37, 38, 39 and 40 as verified by D%. The limit value of D% is 25% (LIEW et al., 2003 cited by VIOLA et al., 2012), more restrictive than that of 55% for Pbias (MORIASI et al., 2007), since it is a reference for watershed modeling, however Pbias is specific for sediments.

Analyzing the data according to R^2 and NSE, for Group 1, values above 0.92 and 0.84 for R^2 and NSE, respectively, were obtained, except for profile 6. For Group 2, values higher than 0.89 and 0.76 were obtained for R^2 and NSE, respectively, with the exception of profile 22. For Group 3, values above 0.88 and 0.72 for R^2 and NSE, respectively, were obtained, except for profiles 33, 34 and 35. With the exception of profiles 2, 6, 22, 33, 34 and 35, which present concentrations below 10 g/L, all other results presented high values, above 0.72 for NSE and above 0.88 for R^2. This shows the efficiency of the proposed method.

The profiles are suitable for RSR, with values below 0.7, except profiles 2, 6, 22, 33, 34 and 35, which have concentrations below 10 g/L.

As for RSME, it was found the highest value of 12.87.

In general, analyzing the set of statistical coefficients, the model was efficient to determine sediment concentration profile in

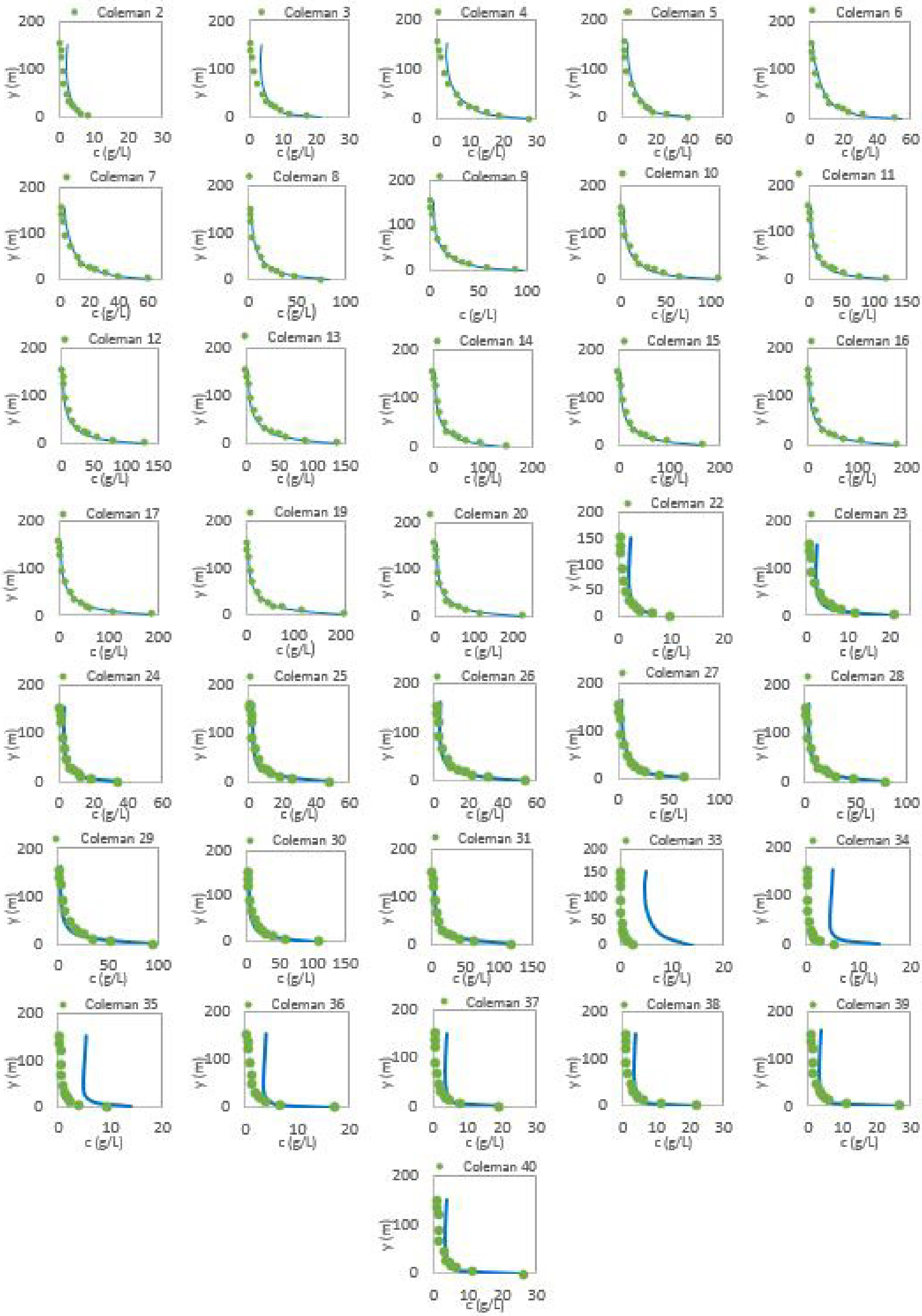

Figure 2. Profiles of sediment concentration measured by Coleman (1981) were identified by points and calculated in this work were identified by the solid lines. Where y (m) is the depth of the fluxo given in meters and c (g / L) the sediment concentration given in g / L.

Table 3. Summary of the results of this work using data from Coleman (1981).

Profile	c measured (g/L)	Parameters		Calculated sediment concentration profile												
		λ_1	a	c estimated (g/L)	D %		Error	NSE		R^2		PBIAS		RSR		RMSE
2	3.3	0.020	1.03 a 8.48	8.9	396.6%	Sup	61.8	-4.24	I	0.99	S	-169%	I	1.54	I	5.65
3	5.7	0.050	1.02 a 4.9	6.5	126.6%	Sup	9.5	0.84	Exc	0.88	S	-14%	S	0.43	S	1.98
4	8.9	0.072	1.03 a 7.63	9.6	74.5%	Sup	8.4	0.97	Exc	0.98	S	-8%	S	0.18	S	1.48
5	12.1	0.085	1.03 a 8.05	12.2	41.7%	Sup	0.3	0.97	Exc	0.98	S	0%	S	0.16	S	1.82
6	15.0	0.100	1.03 a 9.42	14.2	39.3%	Sup	-9.6	0.35	S	0.41	S	5%	S	0.83	I	11.66
7	18.7	0.105	1.03 a 8.94	18.5	20.5%	S	-3.0	0.95	Exc	0.95	S	1%	S	0.22	S	4.04
8	22.3	0.115	1.03 a 8.48	20.8	10.4%	B	-18.1	0.96	Exc	0.96	S	7%	S	0.20	S	4.50
9	25.7	0.122	1.03 a 8.71	24.0	9.8%	MB	-20.7	0.96	Exc	0.97	S	7%	S	0.19	S	5.04
10	29.7	0.130	1.03 a 8.48	26.3	4.7%	MB	-41.7	0.95	Exc	0.96	S	12%	S	0.23	S	7.25
11	32.8	0.138	1.03 a 8.48	29.6	8.3%	MB	-38.9	0.95	Exc	0.97	S	10%	S	0.21	S	7.94
12	34.9	0.139	1.03 a 8.48	31.4	-0.5%	MB	-41.3	0.96	Exc	0.97	S	10%	S	0.20	S	7.70
13	38.4	0.142	1.03 a 8.48	33.2	-5.2%	MB	-62.6	0.94	Exc	0.96	S	14%	S	0.23	S	9.47
14	41.3	0.145	1.03 a 8.48	35.9	-5.4%	MB	-64.3	0.94	Exc	0.96	S	13%	S	0.23	S	10.45
15	43.9	0.150	1.03 a 8.48	38.3	-5.9%	MB	-67.2	0.95	Exc	0.96	S	13%	S	0.22	S	11.22
16	46.3	0.152	1.03 a 8.71	40.8	-4.4%	MB	-66.4	0.95	Exc	0.96	S	12%	S	0.21	S	11.50
17	46.2	0.155	1.03 a 8.48	42.2	-2.0%	MB	-49.0	0.96	Exc	0.97	S	9%	S	0.19	S	10.80
18	47.0	0.156	1.03 a 8.48	42.7	-5.7%	MB	-51.9	0.95	Exc	0.97	S	9%	S	0.20	S	11.40
19	50.3	0.158	1.03 a 8.48	45.7	-1.8%	MB	-55.3	0.96	Exc	0.97	S	9%	S	0.19	S	11.41
20	52.6	0.164	0	45.7	-5.1%	MB	-82.5	0.96	Exc	0.97	S	13%	S	0.19	S	12.87
22	2.8	0.040	1 a 3.32	7.1	416.2%	Sup	47	-4.21	I	0.97	S	-141%	I	1.11	I	4.39
23	5.5	0.058	1 a 3.32	8.1	157.8%	Sup	31.0	0.76	MB	0.96	S	-47%	S	0.48	S	2.83
24	8.5	0.080	1 a 3.04	9.1	78.4%	Sup	7.3	0.97	Exc	0.98	S	-7%	S	0.18	S	1.63
25	11.5	0.100	1 a 3.32	13.2	57.9%	Sup	20.3	0.94	Exc	0.96	S	-15%	S	0.24	S	3.37
26	14.2	0.100	1 a 3.32	13.9	29.2%	Sup	-3.1	0.97	Exc	0.97	S	2%	S	0.18	S	2.78
27	16.9	0.114	1 a 3.32	16.7	26.6%	Sup	-3.0	0.96	Exc	0.97	S	1%	S	0.18	S	3.60
28	19.9	0.122	1 a 3.32	19.6	18.4%	S	-2.7	0.97	Exc	0.97	S	1%	S	0.17	S	3.96
29	22.6	0.130	1 a 3.32	21.9	14.4%	B	-8	0.95	Exc	0.96	S	3%	S	0.20	S	5.74
30	25.2	0.136	1 a 3.32	24.5	10.6%	B	-8.6	0.95	Exc	0.96	S	3%	S	0.21	S	6.86
31	26.9	0.135	1 a 3.52	27.7	14.1%	MB	9.2	0.91	Exc	0.92	S	-3%	S	0.29	S	10.10
33	0.7	0.030	1.02 a 1.59	5.8	1658.7%	Sup	62.4	-57.67	I	0.90	S	-799%	I	1.71	I	5.47
34	1.1	0.030	1.02 a 1.68	5.9	1085.9%	Sup	57.4	-12.19	I	0.92	S	-421%	I	1.56	I	4.92
35	1.9	0.030	1.02 a 1.68	6.0	689.5%	Sup	49.4	-1.83	I	0.95	S	-218%	I	1.28	I	4.16
36	3.2	0.050	1.02 a 1.68	5.3	328.9%	Sup	24.9	0.72	MB	0.95	S	-65%	I	0.55	S	2.41
37	3.8	0.056	1.02 a 1.68	5.4	214.1%	Sup	19.6	0.83	Exc	0.94	S	-43%	S	0.42	S	2.09
38	4.7	0.062	1.02 a 1.68	5.6	150.4%	Sup	10.9	0.86	Exc	0.89	S	-19%	S	0.38	S	2.22
39	5.3	0.072	1.02 a 1.68	6.1	116.7%	Sup	9.3	0.92	Exc	0.93	S	-15%	S	0.29	S	2.04
40	5.2	0.070	1.02 a 1.68	6.0	110.1%	Sup	9.6	0.91	Exc	0.92	S	-15%	S	0.30	S	2.053

Where Exc = Excellent; MB = Very Good; B = Good; S = Satisfactory; Sub = Underestimate; Sup = Overestimate; I = Unsatisfactory. c = concentration of sediments at a vertical distance y; λ1 = Lagrange multiplier, dimensionless; a = parameter related to the characteristics of sediment particles. Nash-Sutcliffe efficiency (NSE); coefficient of determination (R2); Deviation between observed and simulated flows (D%); Pbias; ratio of the root mean square error to the standard deviation of measured data (RSR); e root-mean-square error (RMSE).

all profiles except for profiles 2, 22, 33, 34 and 35, both with low concentrations. Profile 6 was anomalous and did not fit as well.

The simulation performed with Einstein and Chien (1955) is shown in Figure 3 and Table 4. Each RunS is a sediment concentration profile with different velocities and granulometries, detailed in Table 2.

The calibration of the model was performed based on the coefficients of R^2 and NSE. In order to identify the best results, the parameters which brought the highest values of NSE and R^2 were adopted, respectively, to the concentration profile.

The model of the present study did not overestimate or underestimate the sediment concentration of the data of Einstein and Chien (1955) according to D% and Pbias%, contrary to the data obtained by Coleman (1981).

The RSR values were satisfactory for all profiles.

In Table 4 the measured concentrations X estimated concentrations can be visualized. There are acceptable results for NSE and R^2 for all profiles with NSE higher than 0.73 and R^2 higher than 0.81. The cumulative distribution function (CDF) was not well estimated only in the Run6.2 profile. This may be due to the fact that practically the whole profile is in low concentrations.

The comparison of the simulation with the results of Cui (2011) can be visualized in Figure 4 and Table 5. One can observe the adherence of the calculated and measured data.

The square error of RunS1, RunS11 and RunS13 profiles of 65.5; 16.43 and 4269, respectively, calculated in this study were lower than those found by Cui (2011), of 84.17; 21.4 and 47447,

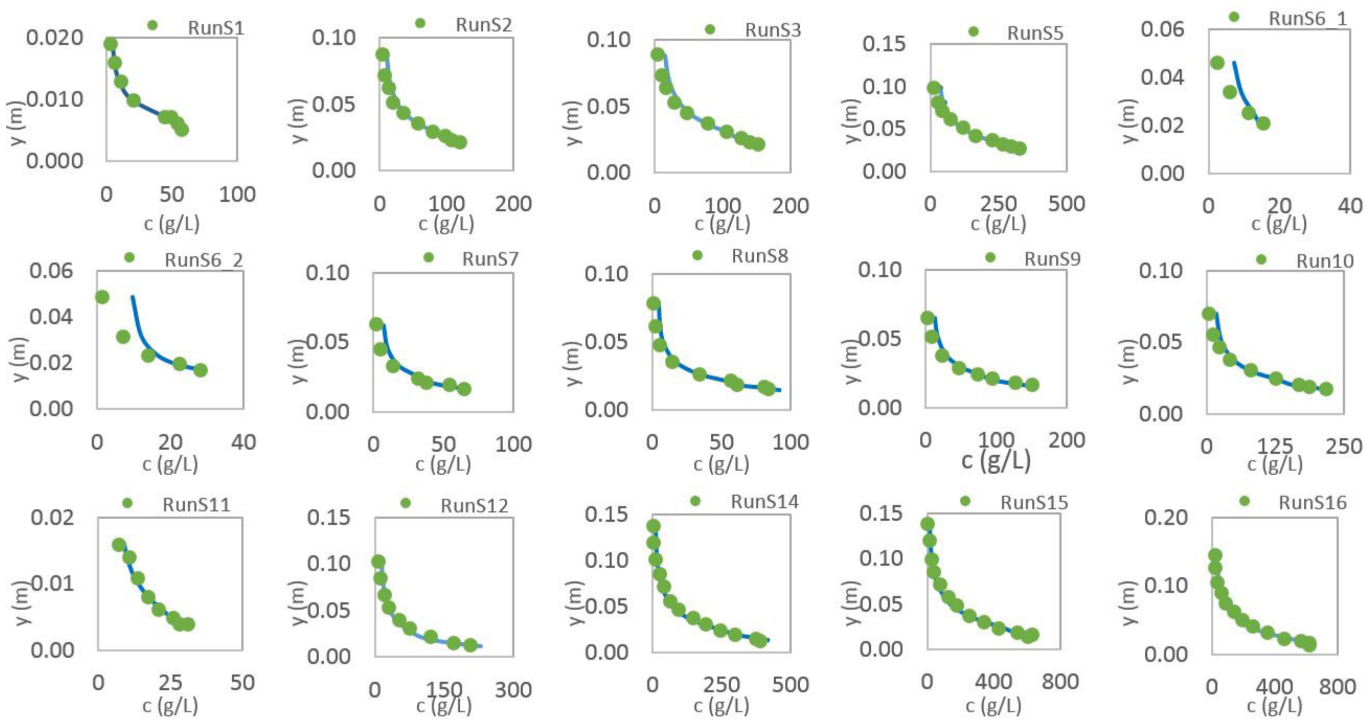

Figure 3. Sediment concentration profiles measured by Einstein and Chien (1955) were identified by points and calculated in this work were identified by the continuous lines. Where y (m) is the depth of the fluxo given in meters and c (g/L) the sediment concentration given in g/L.

Table 4. Summary of the results of this work using data from Einstein and Chien (1955).

Profile	c measured (g/L)	Parameters		Sediment concentration profile calculated												
		λ_1	a	c estimated (g/L)	D %		Error	NSE		R^2		PBIAS		RSR		RMSE
RunS1	34.83	0.29	1.22 a 2.93	30.49	6.4%	MB	-2.92	1.00	Exc	0.983	S	2%	S	0.027	S	0.60
RunS2	59.92778	0.32	1.36 a 3.6	56.27	19.6%	S	19.65	1.00	Exc	0.988	S	-3%	S	0.034	S	1.40
RunS3	77.91111	0.19	1.3 a 2.93	71.86	13.7%	B	12.39	1.00	Exc	0.976	S	-1%	S	0.021	S	1.11
RunS4	106.9867	0.09	1.35 a 2.93	95.77	0.6%	MB	-13.91	1.00	Exc	0.965	S	2%	S	0.016	S	1.18
RunS5	172.2778	0.03	1.03 a 1.59	162.02	12.8%	B	55.53	1.00	Exc	0.998	S	-3%	S	0.022	S	2.36
RunS6_1	11.00333	12	1.48 a 2.37	10.43	15.4%	S	6.54	0.95	MB	0.999	S	-8%	S	0.285	S	1.28
RunS6_2	17.9625	0.2	0.91 a 0.66	16.89	15.3%	S	11.23	0.98	Exc	0.941	S	4%	S	0.170	S	1.50
RunS7	34.49	0.47	1.33 a 2.86	30.17	22.6%	S	2.38	1.00	Exc	0.993	S	0%	S	0.028	S	0.58
RunS8	42.4775	0.45	1.22 a 2.93	37.46	23.8%	S	-3.53	1.00	Exc	0.981	S	2%	S	0.020	S	0.63
RunS9	75.22143	0.11	1.17 a 1.88	67.53	15.4%	S	10.23	1.00	Exc	0.996	S	-1%	S	0.022	S	1.13
RunS10	106.4688	0.09	1.2 a 2.13	98.89	18.7%	S	32.60	1.00	Exc	0.988	S	-3%	S	0.025	S	1.90
RunS11	21.09429	13	1.27 a 2.6	21.25	-1.1%	MB	2.29	1.00	Exc	0.977	S	1%	S	0.061	S	0.53
RunS12	85.95125	1.09	1.17 a 3.91	81.22	21.6%	S	35.62	1.00	Exc	0.985	S	-4%	S	0.029	S	1.99
RunS13	151.4222	0.54	1.19 a 5.55	133.74	7.2%	MB	-29.96	1.00	Exc	0.973	S	3%	S	0.009	S	1.17
RunS14	157.72	0.59	1.19 a 6.27	141.84	22.9%	S	-52.48	1.00	Exc	0.969	S	43%	S	0.015	S	2.01
RunS15	269.6642	0.352	1.2 a 6.39	243.83	23.8%	S	-72.02	1.00	Exc	0.947	S	16%	S	0.011	S	2.35
RunS16	286.1833	0.45	1.18 a 5.44	267.27	18.3%	S	23.86	1.00	Exc	0.962	S	26%	S	0.006	S	1.35

Where Exc = Excellent; MB = Very Good; B = Good; S = Satisfactory; Sub = Underestimate; Sup = Overestimate; I = Unsatisfactory. c = concentration of sediments at a vertical distance y; λ1 = Lagrange multiplier, dimensionless; a = parameter related to the characteristics of sediment particles. Nash-Sutcliffe efficiency (NSE); coefficient of determination (R2); Deviation between observed and simulated flows (D%); Pbias; ratio of the root mean square error to the standard deviation of measured data (RSR); e root-mean-square error (RMSE).

using the Tsallis entropy theory and the Rouse Equation, as can be seen in Table 5.

Cui and Singh (2014) compared the estimation of sediment discharge by the entropy theory by Tsallis and Shannon with the same data from Coleman (1981) and Einstein and Chien (1955). The authors observed that, although there were no significant differences between the results, the Tsallis entropy theory presents more accurate results. In order to improve the results, the authors used correction factors. In the same work, they compared the results with the Prandtl von Karman methods, Rouse equation

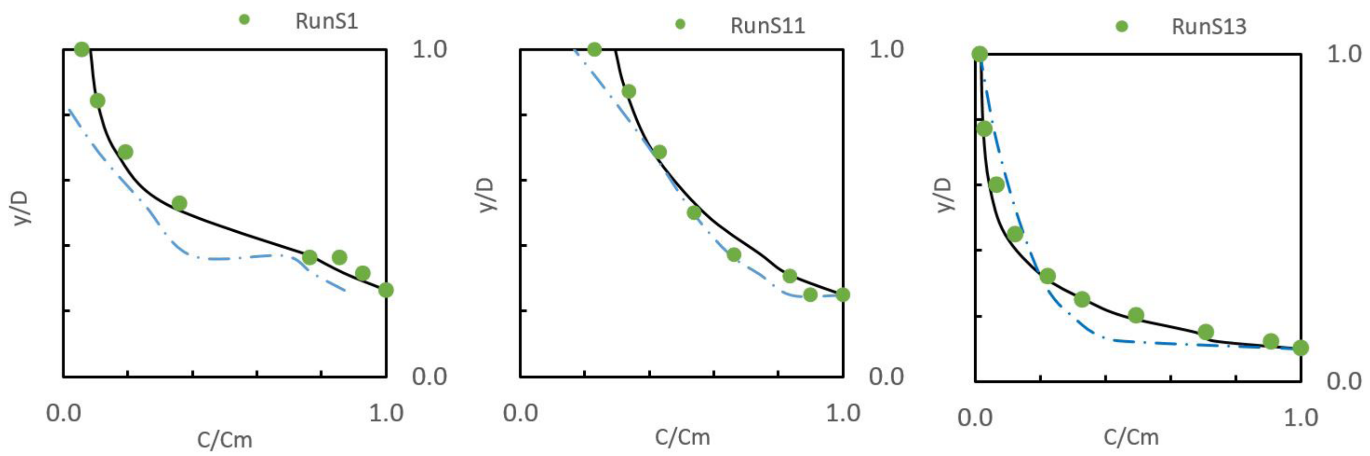

Figure 4. Profile of sediment concentration measured by Einstein and Chien (1955) were identified by points, calculated by Cui (2011) were dashed and in this work by continuous lines. Where y/D is the relation of the depth of the point y by the total depth D, and C/Cm is the ratio of the concentration at the point y by the maximum concentration Cm.

Table 5. Comparison of the estimate of this work with other methods.

Profile	Tsallis			Rouse Equation			In this work		
	Square Error	NSE	R^2	Square Error	NSE	R^2	Square Error	NSE	R^2
RunS1	84.17	0.98	0.98				65.5	0.98	0.98
RunS11	21.4	0.97	0.98	61.33	0.91	0.97	16.43	0.97	0.98
RunS13	47447	0.59	0.79	22910	0.85	0.94	4269	0.97	0.97

Nash-Sutcliffe efficiency (NSE); coefficient of determination (R2).

and found that the methods of estimation of sediment discharge based on the entropy of both Tsallis and Shannon presented better results. Cui (2011) also states that Tsallis's theory represents the sediment concentration profile better than Shannon's. The use of $m = \exp F(c)^{\lambda_1}$ in addition to producing better results, a R^2 higher than Cui (2011) with m = 3, it reduces the number of parameters and consequently the computational effort.

However, Cui (2011) tested the theory of entropy with the methods of Chiu (1987) and Tsallis, and both could represent the low concentrations below 10 g/L better than in the present work. Therefore, a limitation of using the method proposed in this work is the estimation of concentrations below 10 g/L.

It can be verified that it was possible to determine, by the proposed method, the sediment concentration with different velocities and granulometry. The method can be applied for various flow conditions and granulometry above 10 g/L.

CONCLUSION

According to the analysis of results. it can be concluded:

1) It is possible to use the maximum entropy principle to simulate sediment concentration profile under different flow conditions, granulometry and concentration;

2) The use of the relation $m = \exp F(c)^{\lambda_1}$ facilitates calculations, reduces the number of model parameters and consequently computational effort, and better represent the variations of sediment concentration along the profile;

3) The model satisfactorily represents concentrations above 10 g/L;

4) The method can be applied in other estimations, besides sediments, since changes are made in the equation according to the type of parameter to be determined.

REFERENCES

BROWN, C. B. Sediment transport. In: ROUSE, H. (Ed.). *Engineering hydraulics*. New York: Wiley, 1950.

CAPEK, V.; SHEEHAN, D. P. Challenges to the second law of thermodynamics: theory and experiment. In: MERWE, A. V. D. *Fundamental theories of physics*. Denver: University of Denver, 2004. 367 p. v. 146.

CARVALHO, N. O. *Hidrossedimentologia prática*. 2. ed. Rio de Janeiro: Interciência, 2008. 599 p.

CHAO-LIN CHIU, M. Entropy and probability concepts. *Journal of Hydraulic Engineering*, v. 113, n. 5, p. 583-599, 1987. http://dx.doi.org/10.1061/(ASCE)0733-9429(1987)113:5(583).

CHIU, C. L. Entropy and probability concepts in hydraulics. *Journal of Hydraulic Engineering*, v. 113, n. 5, p. 583-599, 1987. http://dx.doi.org/10.1061/(ASCE)0733-9429(1987)113:5(583).

CHIU, C. L. Entropy and 2-D velocity distribution in open channels. *Journal of Hydraulic Engineering*, v. 114, n. 7, p. 738-756, 1988. http://dx.doi.org/10.1061/(ASCE)0733-9429(1988)114:7(738).

CHIU, C. L.; HSU, S. M.; TUNG, N. C. Efficient methods of discharge measurements in rivers and streams based on the probability concept. *Hydrological Processes*, v. 19, n. 20, p. 3935-3946, 2005. http://dx.doi.org/10.1002/hyp.5857.

CHIU, C.; JIN, W.; CHEN, Y. Mathematical models of distribution of sediment concentration. *Journal of Hydraulic Engineering*, v. 126, n. 1, p. 16-23, 2000. http://dx.doi.org/10.1061/(ASCE)0733-9429(2000)126:1(16).

CHIU, C.-L.; JIN, W. Entropy-based modeling and measurement of sediment concentration. In: CONGRESS OF THE INTERNATIONAL ASSOCIATION OF HYDRAULIC RESEARCH, 27., 1997. *Proceedings*... Madrid: IAHR, 1997. p. 1203-1208.

COLBY, B. R.; HEMBREE, C. H. *Computation of total sediment discharge Niobrara River near Cody*. Nebraska: U.S. Geological Survey Water-Supply. 1955. 187 p. Paper 1357.

COLEMAN, N. L. Velocity profiles with suspended on the open-channel distribution. *Water Resources Research*, v. 22, n. 10, p. 1377-1384, 1981. http://dx.doi.org/10.1029/WR022i010p01377.

CONTE, A. E. Entropia e distribuição exponencial simples. In: CONTE, A. E. *Aspectos de um hidrograma máximo mais provável*. São Paulo: Clube de Autores, 2005. p. 29-39.

CUI, H. *Estimation of velocity distribution and suspended sediment discharge in open channels using entropy*. 2011. 212 f. Thesis (Doctoral Dissertation) - Office of Graduate Studies, Texas A&M University, Texas, 2011.

CUI, H.; SINGH, V. P. Suspended sediment concentration in open channels using tsallis entropy. *Journal of Hydrologic Engineering*, v. 19, n. 5, p. 966-977, 2014. http://dx.doi.org/10.1061/(ASCE)HE.1943-5584.0000865.

DESHPANDE, V.; KUMAR, B. Review and assessment of the theories of stable alluvial channel design. *Water Resources*, v. 39, n. 4, p. 481-487, 2013. http://dx.doi.org/10.1134/S0097807812040033.

EINSTEIN, H. A. *The bed load function for sediment transportation in open channels*. Washington: Soil Conservation Service, USDA, 1950. (Technical Bulletin, 1026).

EINSTEIN, H. A.; BARBAROSSA, N. L. River channel roughness. *Transactions of the American Society of Civil Engineers*, v. 117, p. 1121-1132, 1952.

EINSTEIN, H. A.; CHIEN, N. *Effects of heavy sediment concentration near the bed on velocity na sediment distribution*. Berkeley: University of California, 1955. (M. R. D. Sediment Series, 8).

ESPILDORA, B.; AMOROCHO, J. Entropy in the assessment of uncertainty in hydrologic systems and models. *Water Resources Research*, v. 9, n. 6, p. 1511-1522, 1973. http://dx.doi.org/10.1029/WR009i006p01511.

GAN, Y.; DUAN, Q.; GONG, W.; TONG, C.; SUN, Y.; CHU, W.; YE, A.; MIAO, C.; DI, Z. A comprehensive evaluation of various sensitivity analysis methods: a case study with a hydrological model. *Environmental Modelling & Software*, v. 51, p. 269-285, 2014. http://dx.doi.org/10.1016/j.envsoft.2013.09.031.

GOMEZ, B.; PHILLIPS, J. Deterministic uncertainty in bed load transport. *Journal of Hydraulic Engineering*, v. 125, n. 3, p. 305-308, 1999. http://dx.doi.org/10.1061/(ASCE)0733-9429(1999)125:3(305).

HANCOCK, J. C. *An introduction to the principle of communication theory*. New York: McGraw-Hill, 1961. 254 p.

HUSAIN, T. Hydrologic uncertainty measure and network design. *Water Resources Bulletin*, v. 25, n. 3, p. 527-534, 1989. http://dx.doi.org/10.1111/j.1752-1688.1989.tb03088.x.

JAYNES, E. T. Information theory and statistical mechanics. *Information Theory and Statistical Mechanics*, v. 106, p. 620, 1957.

KUMBHAKAR, M.; GHOSHAL, K. One-dimensional velocity distribution in open channels using Renyi entropy. *Stochastic Environmental Research and Risk Assessment*, 2016. In press.

LIEN, H.-P.; TSAI, F.-W. Sediment concentration distribution of debris flow. *Journal of Hydraulic Engineering*, v. 129, n. 12, p. 995-1000, 2003. http://dx.doi.org/10.1061/(ASCE)0733-9429(2003)129:12(995).

LUO, H.; SINGH, V. P. Entropy theory for two-dimensional velocity distribution. *Journal of Hydrologic Engineering*, v. 16, n. 4, p. 303-315, 2011. http://dx.doi.org/10.1061/(ASCE)HE.1943-5584.0000319.

MERTEN, G. H.; MINELLA, J. P. G.; HOROWITZ, A. J.; MORO, M. *Determinação da concentração de sedimentos em suspensão em rios com o uso de turbidímetro*. Porto Alegre: Edição de Gustavo H. Merten, 2014. 97 p.

MINEI, N. *Um método expedito para a medição de vazão em rios e canais abertos*. 1999. 123 f. Thesis (Doctoral Dissertation) - Escola Politécnica, Universidade de São Paulo, São Paulo, 1999.

MOLNAR, P. *Calibration*: watershed modelling, SS. Switzerland: Institute of Environmental Engineering, Chair of Hydrology and Water Resources Management, ETH Zürich, 2011.

MORAMARCO, T.; CORATO, G.; MELONE, F.; SINGH, V. P. An entropy-based method for determining the flow depth distribution in natural channels. *Journal of Hydrology*, v. 497, p. 176-188, 2013. http://dx.doi.org/10.1016/j.jhydrol.2013.06.002.

MORIASI, D. N.; ARNOLD, J. G.; VAN LIEW, M. W.; BINGNER, R. L.; HARMEL, R. D.; VEITH, T. L. Model evaluation guidelines for systematic quantification of accuracy in watershed simulations. *Transactions of the ASABE*, v. 50, n. 3, p. 885-900, 2007. http://dx.doi.org/10.13031/2013.23153.

MUKHOPADHYAY, B.; KHAN, A. Boltzmann-Shannon entropy and river flow stability within Upper Indus Basin in a changing climate. *International Journal of River Basin Management*, v. 13, n. 1, p. 87-95, 2015. http://dx.doi.org/10.1080/15715124.2014.965718.

ONGLEY, E. *Water quality monitoring: a practical guide to the design and implementation of freshwater quality studies and monitoring programmes*.

Geneva: United Nations Environment Programme, World Health Organization, 1996. 15 p.

PAIVA, L. E. D. *A influência do diâmetro representativo do material do leito nas fórmulas de calculo do transporte de sedimentos em escoamentos com superfície 50 livre*. 2007. 384 f. Thesis (Doctoral Dissertation) - Universidade Estadual de Campinas, Campinas, 2007.

POLETO, C.; MERTEN, G. H.; MINELLA, J. P. The identification of sediment sources in a small urban watershed in southern Brazil: An application of sediment fingerprinting. *Environmental Technology*, v. 30, n. 11, p. 1145-1153, 2009. PMid:19947145. http://dx.doi.org/10.1080/09593330903112154.

RESNICK, H. *Fundamentos de física*: mecânica. 8. ed. Rio de Janeiro: LTC, 2008. v. 1.

ROUSE, H. Modern conceptions of the mechanics of turbulence. *Transaction of the. American Society of Civil Engineers*, v. 102, n. 1, p. 463-543, 1937.

SHANNON, C. E. A mathematical theory of communication. *The Bell System Technical Journal*, v. 27, n. 4, p. 623-656, 1948. http://dx.doi.org/10.1002/j.1538-7305.1948.tb00917.x.

SIMONS, D. B.; SENTÜRK, F. *Sediment transport tecnology and water resources publications.* Colorado: Fort Collins, 1992. 897 p.

SING, V. P.; KRSTANOVIC, P. F.; LANE, L. J. *Stochastic models of sediment yield*. Louisian: Elsevier, 1988.

SINGH, V. P. Hydrologic modelling using entropy. *Journal of the Institution of Engineers*, v. 70, p. 55-60, 1989.

SINGH, V. P. The use of entropy in hydrology and water resources. *Issue Hydrological Processes*, v. 11, n. 6, p. 587-626, 1997. http://dx.doi.org/10.1002/(SICI)1099-1085(199705)11:6<587::AID-HYP479>3.0.CO;2-P.

SINGH, V. P. *Entropy-based parameter estimation in hydrology.* Amsterdam: Water Science and Technology Library, 1998.

SINGH, V. P. Hydrologic synthesis using entropy theory. *Journal of Hydrologic Engineering*, v. 16, n. 5, p. 421-433, 2011. http://dx.doi.org/10.1061/(ASCE)HE.1943-5584.0000332.

SINGH, V. P.; CUI, H. Modeling sediment concentration in debris flow by Tsallis entropy. *Physica A*: Statistical Mechanics and its Applications, v. 420, p. 49-58, 2015.

SINGH, V. P.; KRSTANOVIC, P. F. A stochastic model for sediment yield using the principle of maximum entropy. *Water Resources Research*, v. 23, n. 5, p. 781-793, 1987. http://dx.doi.org/10.1029/WR023i005p00781.

SINGH, V. Probability distribution of rainfall-runoff using entropy theory. *Transactions of the ASABE*, v. 55, n. 5, p. 1733-1744, 2012. http://dx.doi.org/10.13031/2013.42364.

SONUGA, J. O. Entropy principle applied to the rainfall-runoff process. *Journal of Hydrology*, v. 30, n. 1-2, p. 81-94, 1976. http://dx.doi.org/10.1016/0022-1694(76)90090-1.

SUBCOMMITTEE ON SEDIMENTATION – SOS. *Determination on fluvial sediment discharge*. Minneapolis: Inter-Agency on Water Resources, 1963. Report. v. 14.

TOFFALETI, F. B. Definitive computations of sand discharge in rivers. *Journal of the Hydraulics Division*, v. 95, n. HY1, p. 225-248, 1969.

TSALLIS, C. Possible generalization of Boltzmann-Gibbs statistics. *Journal of Statistical Physics*, v. 52, n. 1-2, p. 479-487, 1988. http://dx.doi.org/10.1007/BF01016429.

VANONI, V. A. *Sedimentation engineering*. New York: ASCE, 1977.

VIOLA, M. R. C. R.; GIONGO, M.; BESKOW, S.; SANTOS, A. F. Hydrological modeling in a watershed of the Lower Araguaia River Basin, TO. *Journal of Biotechnology and Biodiversity*, v. 3, n. 3, p. 38-47, 2012.

WANG, D.; ZHU, Y. Principle of maximum entropy and its application in hydrology and water resources. *Shui Kexue Jinzhan*, v. 12, n. 3, p. 424-430, 2001.

WEIJS, S. V.; SCHOUPS, G.; VAN DE GIESEN, N. Why hydrological predictions should be evaluated using. *Hydrology and Earth System Sciences*, v. 14, n. 12, p. 2545-2558, 2010. http://dx.doi.org/10.5194/hess-14-2545-2010.

WILLMOTT, C. J.; ACKLESON, S. G.; DAVIS, R. E.; FEDDEMA, J. J.; KLINK, K. M.; LEGATES, D. R.; O'DONNELL, J.; ROWE, C. M. Statistics for evaluation and comparison of models. *Journal of Geophysical Research*, v. 90, n. C5, p. 8995-9005, 1985. http://dx.doi.org/10.1029/JC090iC05p08995.

WORLD METEOROLOGICAL ORGANIZATION – WMO. *Guide to hydrological practices*. Geneva, 1981. v. 168.

XU, G.; ZHAO, L. Analysis of fluvial process based on information entropy. *Journal of Tianjin University Science and Technology*, v. 43, p. 347-353, 2013.

YEVJEVICH, V. *Probability and statistics in hydrology*. Fort Collins: Water Resources Publications, 1972.

Authors contributions

Patrícia Diniz Martins: Confection and analysis of the article.

Cristiano Poleto: Orientation and review of the article.